Characterization of Amm VIII from *Androctonus mauretanicus mauretanicus*: a new scorpion toxin that discriminates between neuronal and skeletal sodium channels

Meriem ALAMI*†, Hélène VACHER*, Frank BOSMANS‡, Christiane DEVAUX*, Jean-Pierre ROSSO*, Pierre E. BOUGIS*, Jan TYTGAT‡, Hervé DARBON§ and Marie-France MARTIN-EAUCLAIRE*[1]

*CNRS UMR 6560, Ingénierie des Protéines, Faculté de Médecine secteur Nord, Institut Jean Roche, Université de la Méditerranée, Bd Pierre Dramard, 13916, Marseille, Cedex 20, France, †Institut Pasteur du Maroc, 1 Rue Abou Kacem Ezzahroui, Casablanca, Morocco, ‡Laboratory of Toxicology, University of Leuven, E. Van Evenstraat 4, 3000, Leuven, Belgium, and §AFMB, CNRS UMR 6098, Chemin Joseph-Aiguier, 13402, Marseille, Cedex 20, France

The venom of the scorpion *Androctonus mauretanicus mauretanicus* was screened by use of a specific serum directed against AaH II, the scorpion α-toxin of reference, with the aim of identifying new analogues. This led to the isolation of Amm VIII (7382.57 Da), which gave a highly positive response in ELISA, but was totally devoid of toxicity when injected subcutaneously into mice. In voltage-clamp experiments with rat brain type II Na^+ channel $rNa_v1.2$ or rat skeletal muscle Na^+ channel $rNa_v1.4$, expressed in *Xenopus* oocytes, the EC_{50} values of the toxin-induced slowing of inactivation were: 29 ± 5 and 416 ± 14 nM respectively for AmmVIII and 2.6 ± 0.3 nM and 2.2 ± 0.2 nM, respectively, for AaH II interactions. Accordingly, Amm VIII clearly discriminates neuronal versus muscular Na^+ channel. The Amm VIII cDNA was amplified from a venom gland cDNA library and its oligonucleotide sequence determined. It shows 87 % sequence homology with AaH II, but carries an unusual extension at its C-terminal end, consisting of an additional Asp due to a point mutation in the cDNA penultimate codon. We hypothesized that this extra amino acid residue could induce steric hindrance and dramatically reduce recognition of the target by Amm VIII. We constructed a model of Amm VIII based on the X-ray structure of AaH II to clarify this point. Molecular modelling showed that this C-terminal extension does not lead to an overall conformational change in Amm VIII, but drastically modifies the charge repartition and, consequently, the electrostatic dipole moment of the molecule. At last, liquid-phase radioimmunassays with poly- and monoclonal anti-(AaH II) antibodies showed the loss of conformational epitopes between AaH II and Amm VIII.

Key words: cDNA, scorpion α-toxin, voltage-activated sodium channel.

INTRODUCTION

Voltage-activated Na^+ channels are the main targets of the toxic polypeptides responsible for the high level of lethality of scorpion venom. The toxins can be broadly divided according to their host specificity: toxins that are active on vertebrates (mammals) and those that are active on invertebrates (arthropods) [1]. They modify the opening or closing of the channels in nerve, muscle and heart cells, thus increasing the depolarization of the membrane and leading to the release of neurotransmitters [2]. Scorpion toxins that are active on vertebrate Na^+ channels can be divided into two types according to their electrophysiological behaviour, differences in their binding sites and ion flux: (i) α-toxins, which slow down the inactivation of the channel and prolong the action potential, and (ii) β-toxins, which cause a shift of the voltage-activated activation to more negative membrane potentials, leading to repetitive firing in both muscles and nerves [3].

Classical α-toxins were the first toxins to be purified and chemically characterized from the scorpion *Androctonus australis* Hector (AaH), a member of the Buthinae from North Africa. These classical α-toxins can be considered to be the only cause of the venom toxicity in this species (90 % of the toxicity for mammals is due to four toxins, AaH I–IV, constituting only 2–3 % of the dry weight of the venom) [4]. The AaH II toxin supports 50 % of the lethal activity in mice and has the highest known affinity for site 3 of the voltage-activated Na^+ channels of excitable cells, where it specifically binds in a membrane-potential-dependent manner [1,3]. Site 3 is formed by the extracellular loops of the α-subunit of the Na^+ channel, between transmembrane segments of domains 1 and 4. Glu^{1613} from the S3–S4 extracellular loop of domain 4 in the α-subunit of the type IIA Na^+ channel (rBII or $rNa_v1.2$) from rat brain is necessary for the α-toxins binding [5,6].

Classical α-toxins are also mainly found in the venoms of *Androctonus mauretanicus mauretanicus* (Amm), *Leiurus quinquestriatus quinquestriatus* (Lqq) and other subspecies of *Buthus* from Africa and Asia [1]. However, Lqq and *Buthus* venoms are particularly rich in closely related molecules, called α-like toxins [3,7]. These α-like toxins are very toxic to both mammals and insects, whereas classical α-toxins are not. They also prolong action potentials in vertebrate and insect electrophysiological preparations but are unable to bind to site 3 on Na^+ channels in rat brain synaptosomes. They differentially affect mammalian central and peripheral excitable cells [8].

The α-like toxins that are highly toxic to insects have been mutated, and some of the structural elements that are important for the receptor recognition in the insect nervous system have been identified [9,10]. Both aromatic and basic residues are involved in this recognition process. The C-terminal amino acids have also been shown to be important [11]. In contrast, there

Abbreviations used: AUFS, absorbance unit full scale; MALDI-TOF, matrix-assisted laser-desorption ionization–time-of-flight; s.c., subcutaneous; i.c.v., intracerebroventricular.

[1] To whom correspondence should be addressed (e-mail eauclaire.mf@jean-roche.univ-mrs.fr).

The nucleotide sequence for Amm VIII has been submitted to the GenBank® Nucleotide Sequence Database under accession number AJ496808.

© 2003 Biochemical Society

is little information concerning the bioactive surface of classical α-toxins, due to the absence of an efficient expression system. Some details were obtained from chemical modifications of α-toxin-specific amino acid residues. These studies suggested that a short segment centred around the Lys^{58} of AaH II plays a major role in the interaction with the receptor. The dramatic decrease in activity observed after the chemical modification of this Lys^{58} was probably related to the loss of an electropositive charge at this position [12].

In this paper, we sought natural analogues of AaH II, the α-toxin of reference, by looking for structural and antigenic similarities in the venom, Amm, of the black scorpion, *A. mauretanicus mauretanicus*, from Morocco. Previous fractionation studies of this venom have identified several of its toxins that are active on different Na^+ or K^+ channels [13–15]. The isolation and characterization of a new toxin, Amm VIII, revealed some structural determinants of the α-toxins, to help us better understand their mechanism of action.

MATERIALS AND METHODS

Materials

Amm scorpions were kept alive in the laboratory. They were a generous gift from the Pasteur Institute in Casablanca, Morocco. Venom was obtained by manual stimulation (100 μl of venom yielded 6 mg of lyophilized protein). The α-toxin of reference, AaH II, Lqq V, Bot III from *Buthus occitanus tunetanus*, Amm V and the non-toxic protein P4 from Amm venom were purified in the laboratory as described previously [4,13]. The following reagents were purchased from the indicated sources: restriction enzymes, DeepVent (exo-) DNA polymerase and Klenow fragment were from New England Biolabs; standard molecular biology reagents were from Sigma and Prolabo; pBluescript SK^+ was from Stratagene; *Escherichia coli* XL1-Blue was from Amersham Biosciences; dNTPs were from Promega; *Pwo* DNA polymerase and carboxypeptidase P were from Roche; DNA purification kits from Qiagen; UV-grade acetonitrile was from Fisons Scientific; trifluoroacetic acid was from Baker. All other analytical reagents were from Merck. BSA was from Sigma. The water used to prepare solvents and buffers was purified with the Milli/Ro/Milli Q system from Millipore. T7 and SP6 mMESSAGE-mMACHINE™ transcription kits were from Ambion; the SMART™ cDNA synthesis kit was from Clontech.

Purification protocols

Amm venom was first purified by gel filtration (two columns of 1.25 cm × 100 cm) through Sephadex G-50 (Pharmacia) in 0.1 M acetic acid. The main toxic fraction was further purified by HPLC on a semi-preparative column (Merck; 4 mm × 250 mm), which had been prepacked with 5 μm Lichrospheres 100 C_8 at 25 °C, using a Waters Associate System as described previously [14]. Solvent A was 0.1 % trifluoroacetic acid and solvent B was acetonitrile/0.1 % trifluoroacetic acid. The linear gradient was from 15 to 38 % solvent B in solvent A for 100 min and from 38 to 80 % solvent B in solvent A for 15 min; the flow rate was 5 ml/min, and the AUFS (absorbance unit full scale) at 215 nm was 1. The fractions of interest were lyophilized and loaded on to a Mono Q HR 5/5 column (Amersham Bioscience) on an FPLC™. A 0–50 % linear gradient of 2 M ammonium acetate, pH 8.5, was applied at a flow rate of 1 ml/min for 60 min; AUFS at 280 nm = 0.15. Amm VIII was then purified by a second run through a Mono Q HR 5/5 column in optimized experimental conditions. We applied 6, 8 and 10 % of 2 M ammonium acetate, pH 8.5, in water in a stepwise manner at a flow rate of 1 ml/min; AUFS at 280 nm = 0.06. Selected fractions were lyophilized and further characterized.

Amino acid sequence determination

Amm VIII (5 nmol) was reduced by dithiothreitol and the cysteines were *S*-alkylated with 4-vinyl-pyridine as described previously [16]. The alkylated peptide was subsequently desalted by C_8-reversed-phase HPLC. An Applied Biosystems 476A sequencer and the recommended programme cycles were used for automatic Edman degradation. Phenylthiohydantoin derivatives were characterized as described previously [15].

MS

Electrospray MS was performed on a Quatro II mass spectrometer (Micromass), as described previously [15,17]. MALDI-TOF (matrix-assisted laser-desorption ionization–time-of-flight) MS was performed on a Perseptive DE-RP (Applied Biosystem) using α-cyano-4-hydroxycinnamic acid as matrix.

Lethality assay in mice

The *in vivo* toxicity of venoms, HPLC fractions or purified toxins was tested by i.c.v. (intracerebroventricular) or s.c. (subcutaneous) injection as described in [14,15]. Experiments were carried out in accordance with the European Communities Council Directive.

Immunization protocols

Immune serum against Amm V was obtained from New Zealand rabbits. Two animals each received 60 μg of protein in Freund's adjuvant (Difco Laboratories) as described previously [18]. Rabbits were first injected intradermally (10 μg) and then s.c. (two injections of 10 μg and two injections of 15 μg) every 3 weeks. Polyclonal (serum 114) and monoclonal (mAb 4C1) antibodies directed against AaH II were obtained and characterized in the laboratory [18,19].

ELISA

Pure toxins (diluted to 7 μg/2 ml) or HPLC fractions were used to coat (100 μl) a 96-well ELISA plate (Nunc Immuno Plate) overnight at 4 °C. After extensive washing, the binding of the specific serum (90 min at room temperature; see the Figures for the dilutions) to the different antigens was measured by incubating with an alkaline phosphatase-coupled goat anti-rabbit Fab (dilution, 1/40 000; Sigma Immuno Chemicals). After 90 min at room temperature the 4-nitrophenyl phosphate substrate was added. After the colour had developed (15 min), the absorbance of each well was measured at 405 nm in a Labsystems iEMS Reader MF.

Radioiodination of the toxins

AaH II and Amm V (1 nmol each) were radio-iodinated using the lactoperoxidase method [12]. The radioactivity was counted using a Packard spectrometer (RIASTAR multidetector system) and was routinely 2000 Ci/mmol.

© 2003 Biochemical Society

RIA

The immunoreactivity of the toxins was assessed by measuring their ability to inhibit the binding of ^{125}I-AaH II or ^{125}I-Amm V to polyclonal and monoclonal antibodies. The appropriate dilution of each antibody for the inhibition tests was determined separately. The dilution resulting in the binding of 50 % of the tracer was used. For the inhibition test, 25 μl of ^{125}I-labelled toxin (final concentrations of 2×10^{-10} M for ^{125}I-AaHII and 4×10^{-10} M for ^{125}I-Amm V) was mixed with 50 μl of one of a series of concentrations of unlabelled toxin and 25 μl of polyclonal antibody (final dilutions of 1/200 000 for antibodies against AaH II and 1/10 000 for antibodies against Amm V) or Protein A–Sepharose purified IgG from mAb 4C1BC5 (which is mAb 4C1 after it had been subcloned for current use; 0.5×10^{-10} M). After incubation for 90 min at 37 °C and then overnight at 4 °C, 0.5 ml of sheep anti-rabbit or anti-mouse precipitating antibody (UCB Bioproducts, Biogenesis) was added. The mixture was incubated for 90 min (with the polyclonal antibodies) or 30 min (with the monoclonal antibodies) at 4 °C and the immune complexes were centrifuged at 10 000 ***g*** for 20 min. All assays were performed in duplicate. The results are expressed as B/Bo, where B and Bo are the radioactivity bound to antibodies in the presence and absence of the unlabelled toxin, respectively.

Expression in *Xenopus* oocytes

For the expression in *Xenopus* oocytes, the rBrainII ($Na_v1.2$)/pLCT1 vector [20] and rSkMI($Na_v1.4$)/pUI-2 vector [21] were linearized with *Not*I and transcribed with the T7 mMESSAGE-mMACHINE kit. The β_1 gene was subcloned into pSP64T [22]. For *in vitro* transcription, β_1/pSP64T was linearized with *Eco*RI. Next, capped cRNA was synthesized from the linearized plasmid using the large-scale SP6 mMESSAGE-mMACHINE transcription kit.

The harvesting of oocytes from anaesthetized female *Xenopus laevis* was as described previously [23]. Oocytes were injected with 50 nl of cRNA at a concentration of 1 ng $\cdot$ nl^{-1} using a Drummond micro-injector. The solution used for incubating the oocytes contained 96 mM NaCl, 2 mM KCl, 1.8 mM $CaCl_2$, 2 mM $MgCl_2$ and 5 mM Hepes (pH 7.4), supplemented with 50 mg $\cdot$ l^{-1} gentamycin sulphate.

Electrophysiological recordings in *Xenopus* oocytes

Two-electrode voltage-clamp recordings were performed at room temperature (18–22 °C) using a GeneClamp 500 amplifier (Axon Instruments) controlled by a pClamp data acquisition system (Axon Instruments). Whole-cell currents from oocytes were recorded 2–4 days after injection. Voltage and current electrodes were filled with 3 M KCl. Resistances of both electrodes were kept as low as possible (< 0.5 MΩ). Bath solution composition was the same as the incubation solution given in the previous section. Using a four-pole low-pass Bessel filter, currents were filtered at 2 kHz and sampled at 10 kHz. Leak and capacitance substraction were performed using a P/4 protocol. Current traces were evoked in an oocyte expressing the cloned sodium channels by depolarizations between -70 and 40 mV, using 10 mV increments, from a holding potential of -90 mV.

Fast inactivation

The degree of fast inactivation was assayed by measuring the I_{5ms}/I_{peak} ratio (rat brain type II Na^+ channel $rNa_v1.2$) or I_{10ms}/I_{peak} (rat skeletal muscle Na^+ channel $rNa_v1.4$), which gives an estimate of the probability for the channels not to be inactivated after 5 ms [24]. Depending on the sodium channel, a test voltage was chosen so that the $I_{5(10)ms}/I_{peak}$ ratio was close to zero under control conditions. $I_{5(10)ms}/I_{peak}$ was measured at the same test voltage after addition of the toxin. Toxin-induced removal of fast inactivation was measured by plotting $I_{5(10)ms}/I_{peak}$ as a function of toxin concentration. The following equation was used:

$$I_{5(10)ms}/I_{peak} = a_0 + \{a_1/[1 + (EC_{50}/[toxin])^h]\}$$

where h is the Hill coefficient, [toxin] is the toxin concentration, a_0 the value of $I_{5(10)ms}/I_{peak}$ obtained at a chosen test voltage under control conditions, where the sum of a_0 and a_1 equals the maximum value of $I_{5(10)ms}/I_{peak}$ at the chosen test voltage indicating the expected maximum effect of the toxin on fast inactivation. Curve manipulations were performed using pClamp8 (Axon Instruments) and Origin software (Microcal).

cDNA amplification and sequence analysis

Total RNA was extracted from the venom glands (48 h after stimulation) by use of guanidinium isothiocyanate/phenol/chloroform extraction, and cDNA was prepared by reverse transcription [25] using the SMART™ cDNA synthesis kit. Based on the coding sequence of the AaH II toxin [26], primer 1 (5′-GTCAACGATATAAACTGCACATAC-3′) corresponded to Val^7–Tyr^{14} of the Amm VIII toxin. The degenerate reverse primer 2 (5′-TKATWYTTAGGATACATTCYWTST-3′) corresponded to the 3′ non coding sequence of the AaH α-toxins [26]. These primer sequences were optimized according to the preferential codon usage in the AaH toxins. The gene encoding Amm VIII was PCR-amplified using 2.5 units of *Pwo* DNA polymerase, 1 μM primer 1 and 2 μM primer 2.

The 5′ region of the Amm VIII cDNA was amplified by PCR using the oligo SMART™ (primer 3; 5′-TACGGCTGCGAGAAGACGACAGAA-3′) and a reverse primer 4 (5′-ACCTTTCAACTTGATACATAGCTCGTT-3′) corresponding to the Asn^{23}–Gly^{31} sequence. PCR amplification was performed using 2.5 units of *Pwo* DNA polymerase and 2 μM of each primer. To amplify the 3′ region of the Amm VIII, a third PCR was performed using forward primer 1 and reverse primer 5 [5′- $(T)_{31}$GCA- 3′]. The PCR amplification was performed using 2.5 units of DeepVent (exo-) polymerase DNA, 1 μM primer 1 and 2.5 μM primer 5. The entire cDNA corresponding to the Amm VIII was obtained with a final PCR amplification, using forward primer 6 (5′-CAATTCATTTTGTCTGCTTTCCTAG-3′) and reverse primer 7 (5′-CTGGATTTAGGATACATTCCATC-3′), which corresponded respectively to the 5′ and 3′ non-coding regions of the Amm VIII cDNA, 2.5 units of *Pwo* DNA polymerase and 1 μM of each primer. For all of the PCR amplification steps, 10 μl of the sample was analysed by 1.2 % agarose-gel electrophoresis in Tris/borate/EDTA buffer, and the PCR products were visualized after ethidium bromide staining. The band of the appropriate size was recovered and purified by 2 % Nusieve GTG agarose-gel electrophoresis in Tris/borate/EDTA buffer and by use of the QIAquick Gel Extraction Kit from Qiagen. When required, the PCR products were blunt-end ligated with dNTPs and the Klenow fragment. The PCR products were cloned into the *Eco*RV site of pBluescript SK$^+$ for sequencing. The plasmid was then propagated in *E. coli* XL1-Blue. The primers designed for amplification were 5′-CGCCAGGGTTTTCCCAGTCACGA-3′ as a forward primer and 5′-AGCGGATAACAATTTCACACAGGA-3′ as reverse primer. The nucleotide sequences of the amplified products were determined using the PE Biosystem ABI Prism model 310 DNA sequencer.

© 2003 Biochemical Society

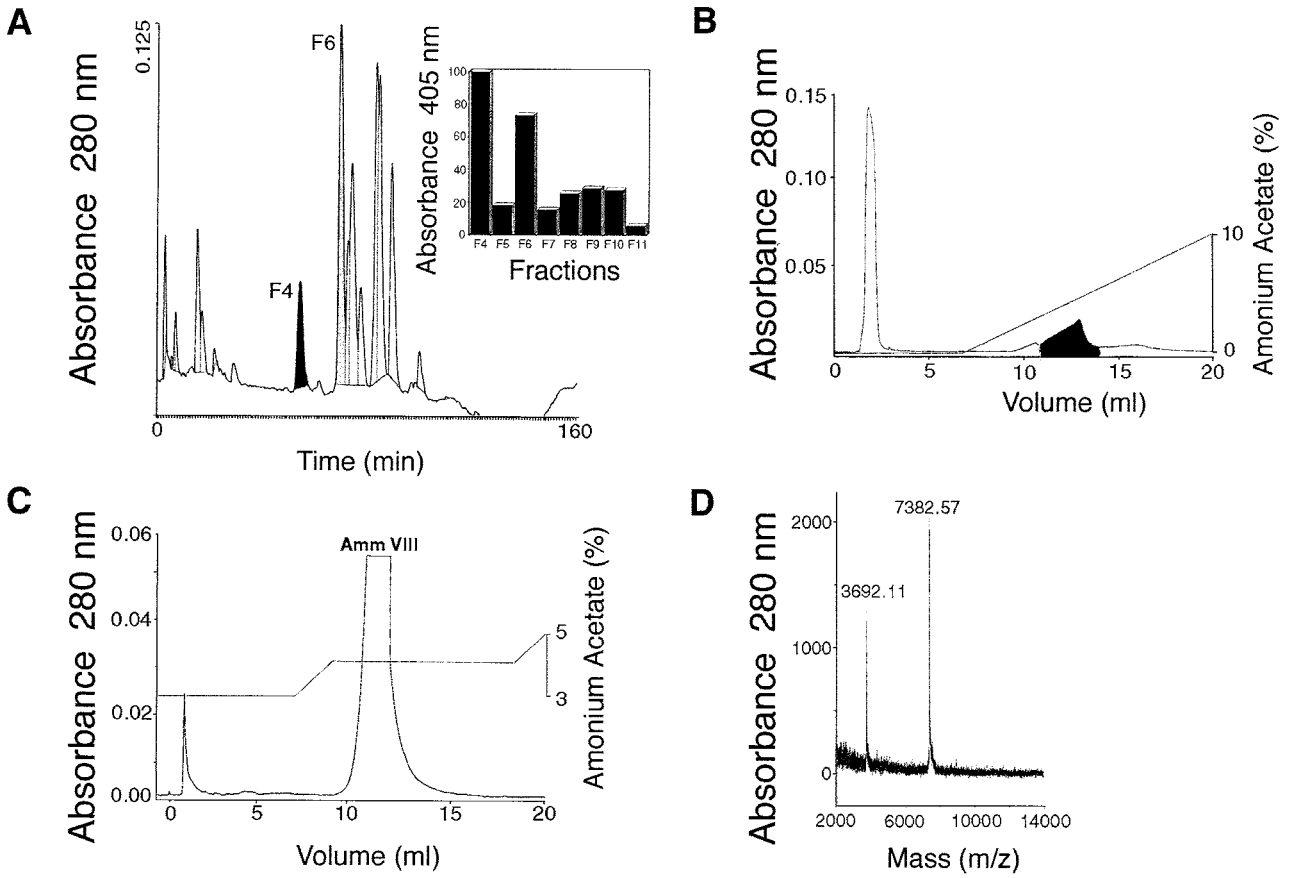

Figure 1 Purification of Amm VIII

(**A**) Reversed-phase HPLC C_8 profile of the soluble Amm venom (100 mg). The components submitted to further purification (numbered F4 and F6) are shown in black and grey, respectively. Inset: ELISA of fractions F4–F11 revealed by a specific serum (dilution 1/10 0000) raised against the α-toxin AaH II. (**B**) Purification of fraction F4 by use of a Mono S FPLC column. The fraction that was further purified is shaded. (**C**) Final purification of Amm VIII (shaded fraction from **B**) by use of a Mono S FPLC column. (**D**) Electrospray MS analysis of Amm VIII.

Molecular modelling

The two toxins Amm V and Amm VIII were modelled based on the known high-resolution X-ray structure of AaH II taking into account the high sequence similarity of these three molecules. Starting from the atomic co-ordinates of AaH II (accession number 1AHO), amino acid residues were changed according to the sequence alignment, keeping the original orientation of the side chains. These preliminary models were then energy-minimized by the Powell conjugate gradient minimizer using the Cartesian co-ordinates as variables and included into the X-PLOR software from the CNS package. All atoms are declared as free, leaving the possibility for the minimizer to change their co-ordinates. Three cycles containing 1000 minimization steps were done, mainly to suppress van-der-Waals distance violations and to find salt bridges and hydrogen bonds while keeping canonical geometries. The program first calculates the total energy of the starting model. The total energy is the sum of the conformational energy terms, which describes the geometry of the model, and the non-bonded energy term, which describes the van-der-Waals and electrostatic energies. The program then attempts to minimize all the energy terms. In the calculation, no water molecules were added. Partial charges were assigned to individual amino acids requested by the CHARMM force field. We used the value of the energy gradient as a convergence criterion: the minimization is run until this value is constantly below 0.5 kcal/mol. Then, the quality of the final model was assessed by the value of the total energy term (-1700 kcal/mol) and the overall geometry was examined by the program PROCHECK. The toxin dipole moment together with the electrostatic calculation and analysis were done using the GRASP software running on a Silicon Graphics workstation, with a charge set that included only the ionizable groups at the N- and C-termini and on amino acid residues Arg, Lys, Asp and Glu [27].

RESULTS

Purification and characterization of Amm VIII

Venom (0.4 g) was first filtered through Sephadex G-50 in 0.1 M acetic acid to separate the components according to their size [28]. One of the fractions (F2) retained 100% of its lethality to mice. MALDI-TOF MS analysis indicated it was composed of molecules ranging from about 3500 to 10000 Da (results not shown). F2 was submitted to reversed-phase HPLC (Figure 1A). ELISA tests were carried out with the HPLC fractions and specific serum against AaH II (Figure 1A, inset). AaH II, which was described as the α-toxin of reference, shares 75% similarity with Amm V, the most potent toxin from Amm venom. The two toxins belong to the same structural α-toxin group (group 2) and Amm V is partly recognized by polyclonal antibodies raised

© 2003 Biochemical Society

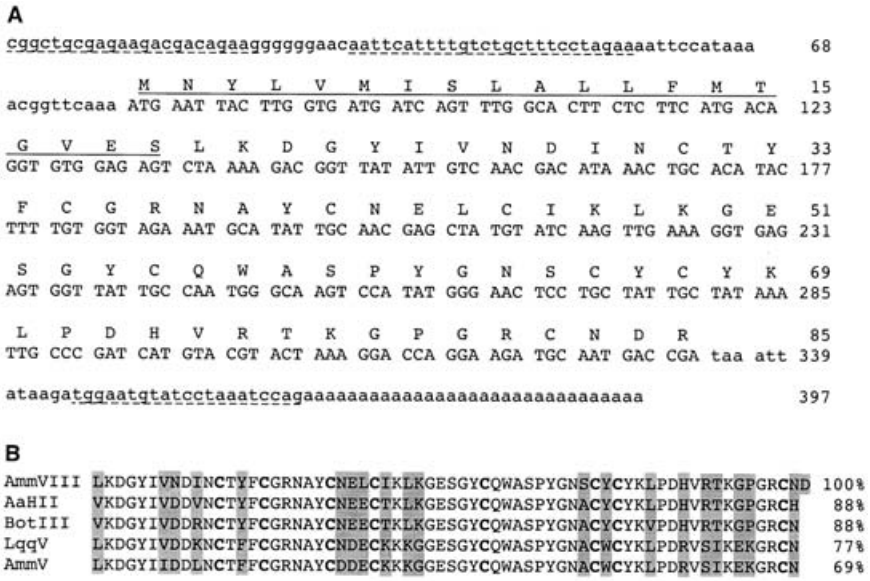

Figure 2 Amino acid sequence of AmmVIII

(**A**) Nucleotide sequence of the cDNA encoding Amm VIII and flanking regions. The predicted amino acid sequence is shown above the nucleotide sequence. Underlined regions correspond to the signal peptide (solid line) and the complementary sequences used as primers (dotted lines; AJ496808). (**B**) Comparison of the amino acid sequences of Amm VIII and four other α-toxins from the same structural group (group 2) that are active on site 3 of voltage-activated Na^+ channels. Sequences were aligned according to the half-cysteine residues (in bold). The residues that differ in all of these toxins are boxed. The similarities were calculated based on the mature toxin, in which the C-terminal residues have been removed following post-translational processing. Sequences were aligned by the ALIGN program from the SBDS package.

Table 1 Bioactivity of Amm VIII and AaH II

	EC_{50}		LD_{50}	
	$rNa_v1.2/\beta_1$	$rNa_v1.4/\beta_1$	Mouse (i.c.v.)	Mouse (s.c.)
Amm VIII	29 ± 5 nM	416 ± 14 nM	225 ng	>1 mg
AaH II	2.6 ± 0.3 nM	2.2 ± 0.2 nM	0.5 ng	0.22 μg

against AaH II [13,14,18]. Two fractions (F4 and F6) were highly immunoreactive. F4 gave a slightly stronger signal than F6. However, F6 was toxic to mice when injected s.c. or i.c.v. whereas F4 was not toxic (up to 20 μg/mouse) when administered by the s.c. route, but was lethal by i.c.v. (1 μg/mouse). MS and Edman degradation showed that F6 contained Amm V (results not shown). F4 was further submitted to FPLC steps on a Mono Q anion exchanger, which led to the isolation of a homogeneous component (Figures 1B and 1C). Its LD_{50} in mice was 225 ng by the i.c.v. route (i.e. 450 times higher than that of AaH II) and no sign of toxicity was observed following s.c. injection (Table 1), even at 1 mg/mouse (i.e. 4000 times higher than that of AaH II).

MS analysis gave a value of 7382.57 Da. Edman degradation of the alkylated protein allowed the identification of the following 61 amino acid residues: LKDGYIVNDINCTYFCGRNAYCNE-LCIKLKGESGYCQWASPYGNSCYCYKLPDHVRXKGPGX-XNX (the identities of the final four residues were uncertain). This sequence is closely related to that of other α-toxins purified from Amm [13,14] and AaH venoms [1,4]. The protein was named Amm VIII, as it is the eighth 'long toxin' to be purified from the venom of Amm [13,14]. Amm VIII constituted 0.023 % of the dry weight of the venom. It is thus in very low abundance compared with other toxins that modulate voltage-activated Na^+ channels and did not contribute to the lethality (by s.c. injection) of the venom.

cDNA amplification and sequence analysis

The amino acid sequence of Amm VIII remained incomplete after Edman degradation. Thus in order to get the missing C-terminal portion, we decided to determine the Amm VIII cDNA oligonucleotide sequence. The degenerate forward primer 1 and the reverse primer 2 were used to amplify the Amm cDNA library transcribed from venom gland mRNA. The PCR yielded a single band of 213 bp. This PCR product was sequenced and encompassed oligonucleotides encoding Val^7 to the 3′ untranslated region of Amm VIII. The 5′ region of the Amm VIII cDNA was amplified using primer 3 and reverse primer 4. A 228 bp band was obtained and sequenced. It gave 50 amino acid residues of the Amm VIII precursor, 19 of which corresponded to a putative signal sequence and 31 of which corresponded to the mature toxin. A third PCR was carried out using forward primer 1 and reverse primer 5 to obtain the 3′ region of the Amm VIII cDNA. A 244 bp band was sequenced. Finally, the entire cDNA (336 bp) encoding the Amm VIII precursor was obtained by a final PCR using forward primer 6 and reverse primer 7 corresponding respectively to the 5′ and 3′ non-coding regions depicted above (accession number AJ496808). The open reading frame encoded 85 amino acid residues corresponding to the Amm VIII precursor (Figure 2A). We assume that the first ATG codon serves as the translation start codon, as a hydrophobic region that is typical of a signal peptide followed it. This signal peptide was identical with that of the α-toxin AaH II. The last residue in the precursor was basic (Arg). A similar residue has also been found in the precursors of other *Androctonus* α-toxins and is further cleaved by carboxypeptidase. It is known that Gly residues allow 'post-translational' α-amidation [25,26]. No Gly residues preceded the Arg residue, indicating that Amm VIII cannot be α-amidated. The Amm VIII amino acid sequence deduced from the cDNA (7384 Da) was consistent with the Amm VIII molecular mass determined by electrospray MS (7382.57 Da). The Amm VIII

© 2003 Biochemical Society

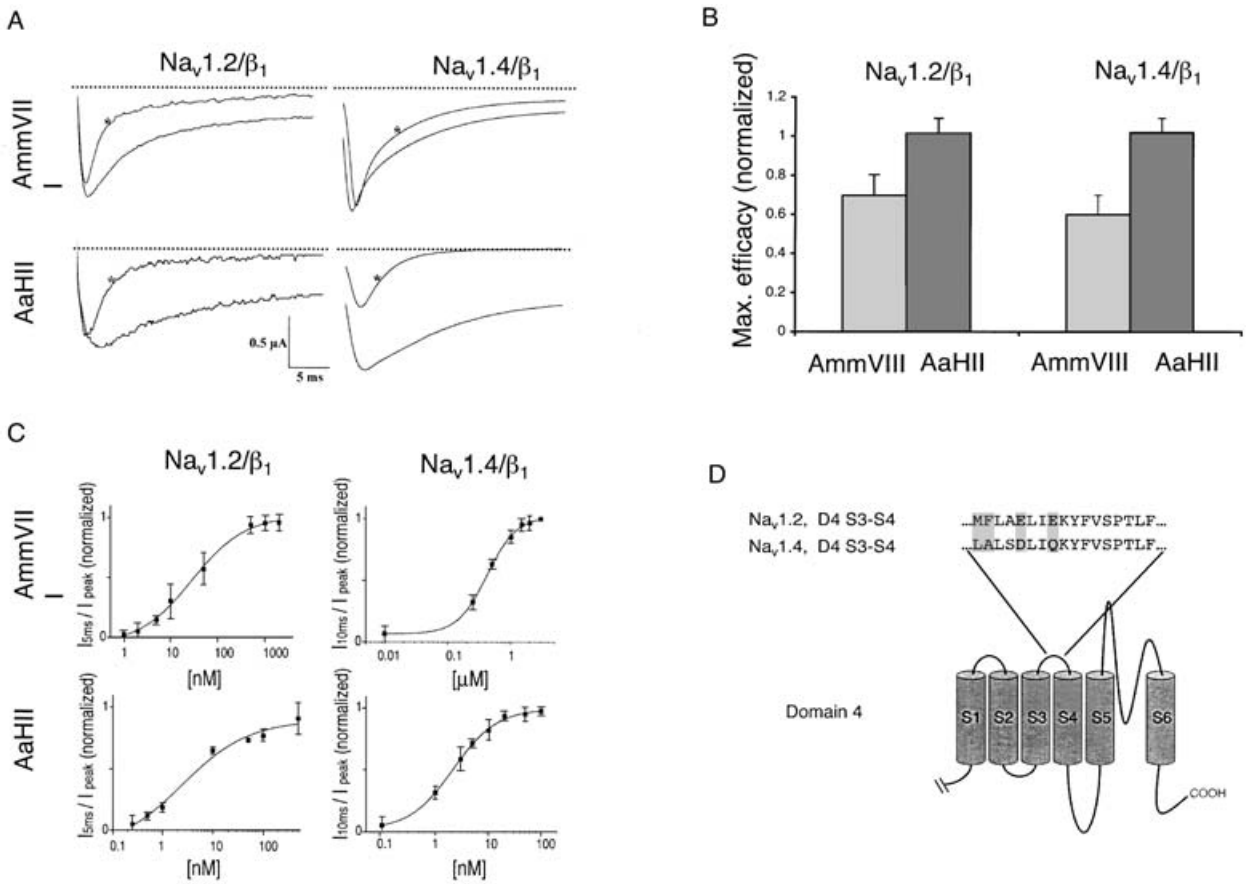

Figure 3 Electrophysiological recordings in *Xenopus* oocytes

(**A**) Left-hand panels show the maximum effect of Amm VIII (500 nM) and AaH II (500 nM) on rNa$_v$1.2/β_1; right-hand panels show the maximum effect of Amm VIII (2 μM) and AaH II (100 nM) on rNa$_v$1.4/β_1 expressed in *X. laevis* oocytes. * represents control conditions were no toxin was added. A clear toxin-induced removal of the inactivation is shown. Current traces were evoked by depolarizations ranging from -20 to 10 mV depending on the Na^+ channel, from a holding potential of -90 mV. (**B**) Histogram indicating the maximal efficacy obtained with Amm VIII and AaH II on the studied voltage-activated Na^+ channels. (**C**) Comparison of the dose-response curves (normalized) of Amm VIII (upper panels) and AaH II (lower panels) on rNa$_v$1.2/β_1 (left-hand panels) and rNa$_v$1.4/β_1 (right-hand panels). Data are means $\pm$ S.E.M. from at least three experiments. (**D**) Amino acid sequences of the transmembrane segment S3–S4 located in domain 4 from rNa$_v$1.2 (residues 1609–1625) or rNa$_v$1.4 (residues 1608–1624). Variable amino acids are shaded.

amino acid composition and molecular mass were found to be similar to those of the non-toxic protein P4, purified previously from Amm venom [13]. So far, the amino acid sequence and the immunological properties of P4 remain undetermined. Thus P4 (7382.47 Da) was submitted to Edman degradation and ELISA tests using specific serum against AaH II (results not shown). After these experiments, it was clear that P4 and Amm VIII are the same molecule. Its complete final sequence was compared with those of the other scorpion α-toxins that belong to the same structural group 2 (Figure 2B). These toxins all bind to site 3 of the voltage-activated Na^+ channels with high affinity and are all highly toxic in mouse by both i.c.v. and s.c. injection [1,7,29]. Amm VIII and AaH II were more similar (88 % sequence homology) than Amm VIII and Amm V (69 %). The main difference was the extra C-terminal acidic residue (Asp) only found in Amm VIII. However, two other mutations involving charged amino acid residues susceptible to impair activity were additionally observed: Asn^8 instead of Asp^8 and Leu^{25} instead of Glu^{25}.

Electrophysiological studies

To better understand the differences in toxicity according to the mode of injection, the actions of Amm VIII and AaH II were further investigated on the rat sodium channel α-subunit from brain rBrainII (rNa$_v$1.2) and skeletal muscle rSkMI (rNa$_v$1.4) co-expressed in oocytes with the β_1 subunit. As shown in Figures 3(A) and 3(B), Amm VIII and AaH II display different efficacies on rNa$_v$1.2/β_1 and rNa$_v$1.4/β_1. The maximal toxin-induced slowing of inactivation caused by addition of Amm VIII is significantly less than the effect of AaH II. Figure 3(A) shows the maximum effect obtained by applying very high doses on the oocytes expressing the voltage-activated Na^+ channels in order to see the maximal effect. To clarify Figure 3(A), Figure 3(B) shows the significant difference between the maximal toxin-induced effects of the two toxins on the two voltage-activated Na^+ channels.

Figure 3(C) shows the concentration dependence of the slowing of inactivation induced by Amm VIII and AaH II on the tested voltage-activated Na^+ channels. EC_{50} values were obtained after a sigmoidal fit of the data and are listed in Table 1. It should be noted that AaH II is 10 times more potent on rNa$_v$1.2/β_1 than Amm VIII and 200 times more potent on rNa$_v$1.4/β_1. Amm VIII is significantly less potent on the studied voltage-activated Na^+ channels and exhibits a lower efficacy than AaH II, in particular on the skeletal muscle Na^+ channel. Figure 3(D) shows the amino acid differences of the transmembrane segment S3–S4 in the domain 4 from rNa$_v$1.2 (P04775) and the homologous segment from rNa$_v$1.4 (P15390) [20,21].

© 2003 Biochemical Society

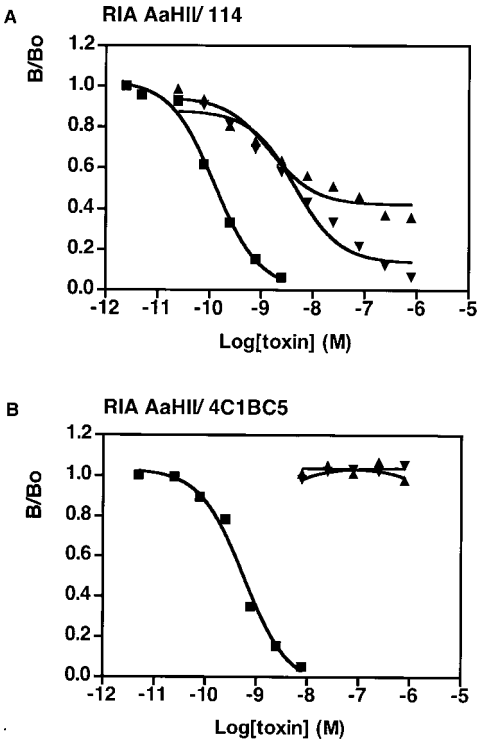

Figure 4 Competitive liquid RIA

(**A**) Inhibition of the binding of ^{125}I-AaH II to polyclonal anti-(AaH II) antibodies (serum 114) by AaH II (■; 10^{-8}–10^{-12} M), AmmVIII (▲) and AmmV (▼; 10^{-6}–10^{-11} M). (**B**) Inhibition of the binding of ^{125}I-AaH II to mAb 4C1BC5 anti-(AaH II) by AaH II (■; 10^{-8}–10^{-12} M), AmmVIII (▲) and AmmV (▼; 10^{-6}–10^{-11} M).

Immunological studies

The antigenic properties of Amm VIII and Amm V were investigated and compared in competitive liquid-phase RIA. The ability of Amm VIII and Amm V to inhibit the binding of ^{125}I-AaH II to polyclonal or monoclonal anti-(AaH II) antibodies was first determined (Figure 4A). Amm V fully inhibited the binding of ^{125}I-AaH II to its polyclonal antibodies (serum 114), but Amm VIII did not. The IC_{50} value was 8×10^{-9} M for Amm V compared with 2×10^{-10} M for native AaH II. Even at a 1 μM concentration, Amm VIII was only able to displace 60 % of the total bound ^{125}I-AaH II. This could be interpreted as a loss of antigenic sites [30]. The monoclonal antibody mAb 4C1 (IC_{50} value, 5.8×10^{-10} M for AaH II) was unable to recognize Amm VIII or Amm V (Figure 4B).

To further define the immunological properties of Amm V and Amm VIII, a rabbit antiserum was raised against Amm V (the most potent and the most represented toxin in the venom). ELISA showed that the serum was able to recognize both Amm V and Amm VIII, although with a slight difference in reactivity (Figure 5A). RIA using ^{125}I-Amm V (0.4 nM) and serial dilutions of the anti-(Amm V) serum showed that the titre was 1/10000 (Figure 5B). The avidity and specificity of the anti-(Amm V) serum were also tested by RIA, which was designed to test the ability of different competitors to inhibit the binding of ^{125}I-Amm V to its specific serum (Figure 5C). Amm V and Lqq V completely inhibited the binding of anti-(Amm V) antibodies to ^{125}I-Amm V. The IC_{50} values were 5×10^{-11} M for Amm V and 2×10^{-10} M for Lqq V. Amm VIII and AaH II were only able to inhibit 30 % of the binding of anti-(Amm V) antibodies to ^{125}I-Amm V.

DISCUSSION

Seven different toxins have previously been purified from the venom of the Moroccan scorpion *Androctonus mauretanicus*. These toxins were easy to identify because of their lethality to mammals via the s.c. route (72.5 % of the total venom toxicity) [13,14]. Alternatively, antibodies specific for the α-toxin of reference, AaH II, were used in this study to detect Amm VIII, which is totally innocuous for mice when administered by the s.c. route. Amm VIII had an additional acid residue, Asp^{65}, which is unusual compared with the other α-toxins. On toxin genes, this may result from a single mutation of the codon GGC (Gly, which allows C-terminal α-amidation) into GAC (Asp). This extra C-terminal residue can induce steric hindrance with the receptor site, as demonstrated for K^+ channel blockers [27]. Also, adding two negative charges at the C-terminal end may induce an overall conformational change responsible for the dramatic reduction in activity, but the modelling did not propose such a change of the interaction surface (Figure 6A). The conformational change induced by additional negative charges is most probably strictly restricted on the C-terminal end.

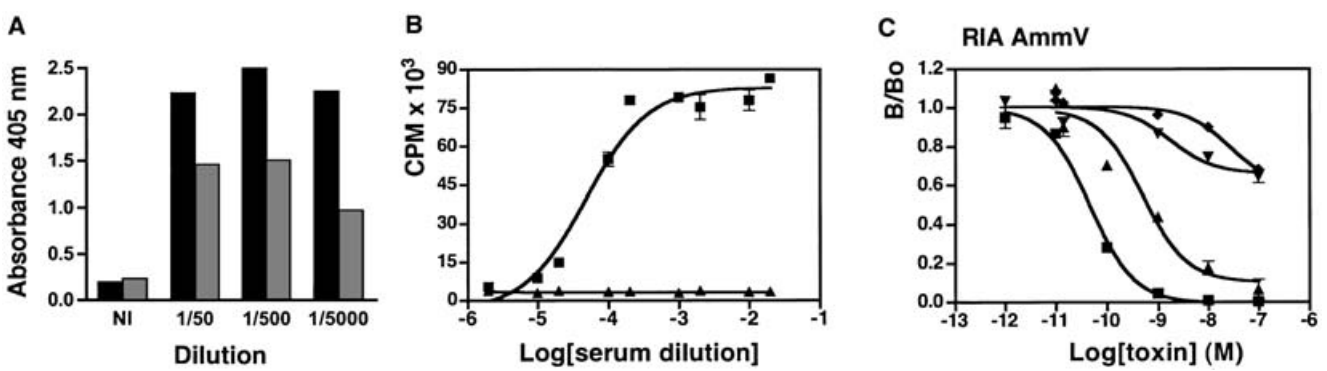

Figure 5 Immunogenic properties of Amm V and Amm VIII

(**A**) ELISA using Amm V (black bars) and Amm VIII (grey bars)-coated plates and specific serum (dilution 1/10000) raised against Amm V. NI is non-immune serum, the negative control. (**B**) Binding of ^{125}I-Amm V (at 0.4 nM) to its specific IgG (■). The non-immune serum (▲) was used as a negative control. (**C**) Competitive liquid RIA between ^{125}I-Amm V bound to its specific IgG and increasing concentrations of Amm V (■), Lqq V (▲), AaH II (●) and Amm VIII (▼).The results are expressed as the ratio B/Bo, where B and Bo are the radioactivity bound to antibodies in the presence and absence of the unlabelled toxin, respectively.

© 2003 Biochemical Society

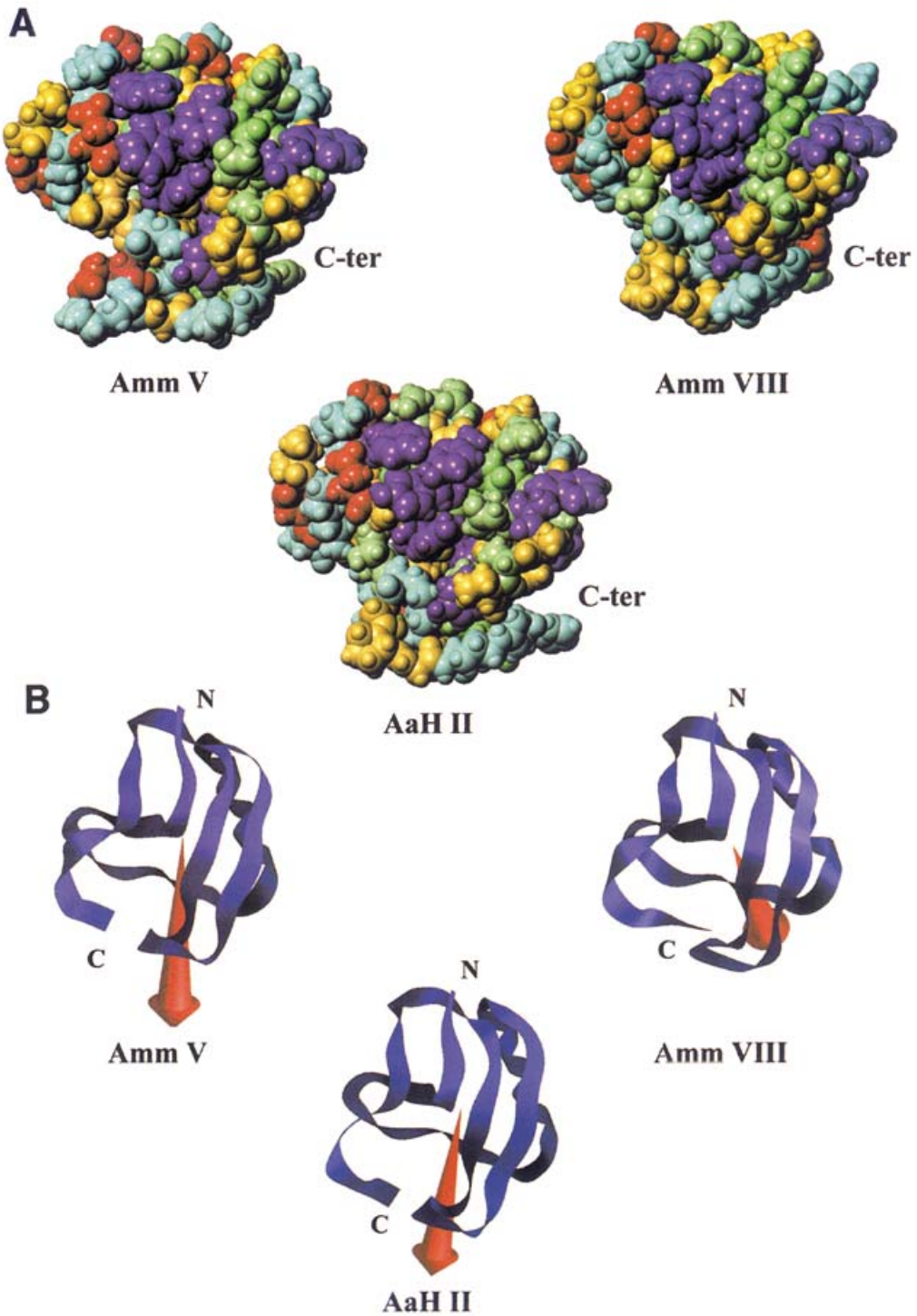

Figure 6 Molecular modelling

(**A**) Space-filling representation of Amm V and Amm VIII compared with AaH II used as a modelling template. Residues are coloured according to the physicochemical characteristics of their side chain: red, acidic; blue, basic; purple, aromatic; green, alcohols and sulphur-containing residues; yellow, aliphatic. (**B**) MOLSCRIPT representation of the backbone conformation of Amm V and Amm VIII modelled on the basis of AaH II. Red arrows indicate the orientation and intensity of dipole moments resulting from electrostatic anisotropy.

However, other different local modifications could explain why Amm VIII behaves differently from AaH II. Scorpion toxins show two flat opposite faces. One face (A) contains a highly conserved aromatic cluster and the opposite face (B) contains a number of charged residues (most of them exposed to the solvent) [31,32]. Two other mutations, involving charged amino acid residues, cause impaired activity (Asn^{8} instead of Asp^{8} and Leu^{25} instead of Glu^{25}). They undoubtedly modify the negative surface of the B

© 2003 Biochemical Society

face of the toxin [32,33], whereas the acidic C-terminal extension disrupts the large positive surface on the hydrophobic face A comprising most of the C-terminal residues of AaH II.

Previous biochemical experiments [11,12,34] and site-directed mutagenesis [9,10,35] suggested that the reverse turn 8–12 and the C-terminal residues 58, 62, 63 and 64 play a major role in the interaction between α-toxins and their receptor. The charged residues in the N- and C-terminal regions probably contribute to the high efficacy of the binding. Lys^{58}, which was shown of fundamental importance for AaH II bioactivity, was also present in Amm VIII. However, as demonstrated by the resulting orientation of the electrostatic dipole moment (Figure 6B), the overall charge repartition is drastically modified in Amm VIII, which is probably more crucial than global charge for toxin binding. The side-chain carboxylate group of the extra C-terminal Asp^{65} is involved in a salt bridge with Arg^{62} in Amm VIII. This salt bridge decreases the availability of the guanidinium group of Arg^{62}, which was reported involved in the binding of AaH II to its receptor site [35]. Additionally, changing Asp^{8} in AaH II into Asn^{8} leads to the formation of a hydrogen bond between the amino group of Asn^{8} and the carboxylate group of Asp^{9} in Amm VIII. This modification is in the 8–12 loop, which may be also involved in the binding of α-toxins to their receptor site [10].

At last, the modification of residue Glu^{25} of AaH II (replacement of a hydrophilic residue by a hydrophobic residue) cannot be directly responsible for the decrease in activity, but may destabilize the α-helix, therefore modifying antibody-recognition properties.

Since Amm VIII is devoid of lethality in mice by s.c. injection, it may constitute a potential natural anatoxin. Its antigenic properties were first compared with those of AaH II, and then with those of Amm V, the toxin responsible of 47% of the lethal activity in the Amm venom [14]. It was previously shown that toxins from the same group are fully cross-reactive in liquid-phase RIA when sequence homology is greater than 75%. However, only a partial cross-reactivity was observed when critical substitutions affected a common antigenic site [30]. Four major antigenic sites have been localized on AaH II. They are considered to be conformational [30,36]. Three sites essentially coincide with turn structures and one is found on the α-helix. The most antigenic regions show potentially increased flexibility, like sequences 5–14, which are linked to 60–64 by a disulphide bridge. In this study, using polyclonal anti-(AaH II) antibodies, at least one epitope seems lost. The amino acids involved in this epitope may be, at least partly, localized in the α-helix or the C-terminal dipeptide. The monoclonal mAb 4C1 did not detect any cross-reactivity between AaH II, Amm VIII and Amm V. The side chains of residues Val^{10}, Lys^{58}, His^{54} and His^{64} of AaH II are thought to play a special role in the recognition of the conformational epitope on AaH II by mAb 4C1 [19]. In Amm VIII and Amm V, Ile^{10} and Leu^{10} replace Val^{10} respectively and Asn^{64} replaces His^{64} in both toxins. Moreover, Arg^{54} in Amm V replaces His^{54} and there is an extra Asp^{65} in Amm VIII. These changes may explain why Amm VIII and Amm V are not recognized at all by mAb 4C1. Taken together, our results indicate that there is a dominant immunogenic domain in the C-terminal region of Amm V and Amm VIII, as has been suggested previously for AaH II. Two antigenic sites, one around the 12–63 disulphide bridge, the other encompassing residues 50–59, are involved in AaH II neutralization [30,37]. Thus this domain is of particular interest for the immunotherapy of scorpionism.

The EC_{50} values of the slowing of inactivation induced by the α-toxin of reference AaH II on $rNa_v1.2$ or $rNa_v1.4$ expressed in *Xenopus* oocytes with the β_1-subunit are in the same range as those established with solely the α-subunit of the channels [38]. By using site-directed mutagenesis, the extracellular loop S3–S4 in the domain 4 of the $rNa_v1.2$ α-subunit has been identified as part of the α-toxin Lqq V receptor site 3 [6,39]. AaH II and Amm VIII presumably also bind to the channel isoforms at the domain 4 S3–S4 linker region, with widely differing affinities. Our results demonstrate that $rNa_v1.4$ is more resistant to Amm VIII than $rNa_v1.2$, suggesting that modification in the domain 4 S3–S4 linker of $rNa_v1.4$ is sufficient to confer this resistance. Interestingly, while the conserved residue Asp into the homologous site of rNav1.4 replaces $rNa_v1.2$-Glu^{1613}, the neutral residue Gln in $rNa_v1.4$ replaces the $rNa_v1.2$-Glu^{1616} (Figure 3D). This mutation does not reduce the sensitivity of $rNa_v1.4$ to AaH II, but, on the contrary, decreases the Amm VIII binding. These results strongly suggest that, in our study, Amm VIII discriminates between neuronal and skeletal sodium channel isoforms by recognizing the difference in a single anionic residue in the receptor-binding site. However, previous studies using neuronal Na^+ channels have also implicated other extracellular loops in domains D1 and D4 as contributors to the α-toxin-binding site-3 [6–8]. At present, little is known about the quaternary structure of the Na^+ channels, and it is reasonable to assume the possible involvement of distinct outside regions in the α-toxin-binding process.

We thank the Pasteur Institute from Morocco and Professor A. Benslimane for generously providing the Amm venom and the living animals. We thank the following persons: Professor A. L. Goldin (University of California, Irvine, CA, U.S.A.) for sharing $rNa_v1.2$, Professor G. Mandel (State University of New York, New York, U.S.A.) for sharing $rNa_v1.4$ and Professor S. H. Heinemann (Friedrich-Schiller-Universität Jena, Germany) for sharing the β_1 subunit. We also thank R. Ouguideni, S. Canarelli and Dr B. Céard for their technical assistance with the oligonucleotides and amino acid sequencing and Dr P. Mansuelle for expert interpretation of amino acid sequence and MS data. M. A. was supported by the World Health Organisation and by the Société de Secours des Amis des Sciences. H. V. was supported by the Délégation Générale pour l'Armement. This paper is dedicated to the memory of Dr H. Zerrouk, who contributed greatly to the study of Amm venom.

REFERENCES

1 Martin, M. F. and Couraud, F. (1995) Scorpion neurotoxins: effects and mechanisms. In Handbook of Neurotoxicology (Chang, L. W. and Dyer, R. S., eds.), pp. 683–716, Marcel Dekker, New York
2 Catterall, W. A. (1992) Cellular and molecular biology of voltage-activated sodium channels. Physiol. Rev. **72**, S15–S48
3 Cestele, S. and Catterall, W. A. (2000) Molecular mechanisms of neurotoxin action on voltage-activated sodium channels. Biochimie **82**, 883–892
4 Martin, M. F. and Rochat, H. (1986) Large scale purification of toxins from the venom of the scorpion *Androctonus australis* Hector. Toxicon **24**, 1131–1139
5 Thomsen, W. J. and Catterall, W. A. (1989) Localization of the receptor site for alpha-scorpion toxins by antibody mapping: implications for sodium channel topology. Proc. Natl. Acad. Sci. U.S.A. **86**, 10161–10165
6 Rogers, J. C., Qu, Y., Tanada, T. N., Scheuer, T. and Catterall, W. A. (1996) Molecular determinants of high affinity binding of alpha-scorpion toxin and sea anemone toxin in the S3-S4 extracellular loop in domain IV of the Na^+ channel alpha subunit. J. Biol. Chem. **271**, 15950–15962
7 Gordon, D., Martin-Eauclaire, M. F., Cestele, S., Kopeyan, C., Carlier, E., Khalifa, R. B., Pelhate, M. and Rochat, H. (1996) Scorpion toxins affecting sodium current inactivation bind to distinct homologous receptor sites on rat brain and insect sodium channels. J. Biol. Chem. **271**, 8034–8045
8 Gilles, N., Chen, H., Wilson, H., Le Gall, F., Montoya, G., Molgo, J., Schonherr, R., Nicholson, G., Heinemann, S. H. and Gordon, D. (2000) Scorpion alpha and alpha-like toxins differentially interact with sodium channels in mammalian CNS and periphery. Eur. J. Neurosci. **12**, 2823–2832
9 Zilberberg, N., Gordon, D., Pelhate, M., Adams, M. E., Norris, T. M., Zlotkin, E. and Gurevitz, M. (1996) Functional expression and genetic alteration of an alpha scorpion neurotoxin. Biochemistry **35**, 10215–10222
10 Zilberberg, N., Froy, O., Loret, E., Cestele, S., Arad, D., Gordon, D. and Gurevitz, M. (1997) Identification of structural elements of a scorpion alpha-neurotoxin important for receptor site recognition. J. Biol. Chem. **272**, 14810–14816

© 2003 Biochemical Society

11 Martin, M. F., Vargas, O. and Rochat, H. (1989) Importance of the C-terminal amino acid residues on scorpion toxins activity. In Second forum on peptides (Aubry, A., Marraud, M. and Vitous, B., eds.), pp. 483–486, John Libbey Eurotext, Paris

12 Darbon, H., Jover, E., Couraud, F. and Rochat, H. (1983) Alpha-scorpion neurotoxin derivatives suitable as potential markers of sodium channels. Preparation and characterization. Int. J. Pept. Protein. Res. **22**, 179–186

13 Rosso, J. P. and Rochat, H. (1985) Characterization of ten proteins from the venom of the Moroccan scorpion *Androctonus mauretanicus mauretanicus*, six of which are toxic to the mouse. Toxicon **23**, 113–125

14 Zerrouk, H., Bougis, P. E., Ceard, B., Benslimane, A. and Martin-Eauclaire, M. F. (1991) Analysis by high-performance liquid chromatography of *Androctonus mauretanicus mauretanicus* (black scorpion) venom. Toxicon **29**, 951–960

15 Crest, M., Jacquet, G., Gola, M., Zerrouk, H., Benslimane, A., Rochat, H., Mansuelle, P. and Martin-Eauclaire, M. F. (1992) Kaliotoxin, a novel peptidyl inhibitor of neuronal BK-type Ca^{2+} -activated K^+ channels characterized from *Androctonus mauretanicus mauretanicus* venom. J. Biol. Chem. **267**, 1640–1647

16 Romi-Lebrun, R., Lebrun, B., Martin-Eauclaire, M. F., Ishiguro, M., Escoubas, P., Wu, F. Q., Hisada, M., Pongs, O. and Nakajima, T. (1997) Purification, characterization, and synthesis of three novel toxins from the Chinese scorpion *Buthus martensi*, which act on K^+ channels. Biochemistry **36**, 13473–13482

17 Hassani, O., Loew, D., Van Dorsselaer, A., Papandreou, M. J., Sorokine, O., Rochat, H., Sampieri, F. and Mansuelle, P. (1999) Aah VI, a novel, N-glycosylated anti-insect toxin from *Androctonus australis* hector scorpion venom: isolation, characterisation, and glycan structure determination. FEBS Lett. **443**, 175–180

18 El Ayeb, M., Delori, P. and Rochat, H. (1983) Immunochemistry of scorpion alpha-toxins: antigenic homologies checked with radioimmunoassays (RIA). Toxicon **21**, 709–716

19 Bahraoui, E., Pichon, J., Muller, J. M., Darbon, H., Elayeb, M., Granier, C., Marvaldi, J. and Rochat, H. (1988) Monoclonal antibodies to scorpion toxins. Characterization and molecular mechanisms of neutralization. J. Immunol. **141**, 214–220

20 Noda, M., Ikeda, T., Kayano, T., Suzuki, H., Takeshima, H., Kurasaki, M., Takahashi, H. and Numa, S. (1986) Existence of distinct sodium channel messenger RNAs in rat brain. Nature (London) **320**, 188–192

21 Trimmer, J. S., Cooperman, S. S., Tomiko, S. A., Zhou, J. Y., Crean, S. M., Boyle, M. B., Kallen, R. G., Sheng, Z. H., Barchi, R. L. and Sigworth, F. J. (1989) Primary structure and functional expression of a mammalian skeletal muscle sodium channel. Neuron **3**, 33–49

22 Gellens, M. E., George, Jr, A. L., Chen, L. Q., Chahine, M., Horn, R., Barchi, R. L. and Kallen, R. G. (1992) Primary structure and functional expression of the human cardiac tetrodotoxin-insensitive voltage-activated sodium channel. Proc. Natl. Acad. Sci. U.S.A. **89**, 554–558

23 Liman, E. R., Tytgat, J. and Hess, P. (1992) Subunit stoichiometry of a mammalian K^+ channel determined by construction of multimeric cDNAs. Neuron **9**, 861–871

24 Chen, H., Lu, S., Leipold, E., Gordon, D., Hansel, A. and Heinemann, S. H. (2002) Differential sensitivity of sodium channels from the central and peripheral nervous system to the scorpion toxins Lqh-2 and Lqh-3. Eur. J. Neurosci. **16**, 767–770

25 Alami, M., Ouafik, L., Ceard, B., Legros, C., Bougis, P. E. and Martin-Eauclaire, M. F. (2001) Characterisation of the gene encoding the alpha-toxin Amm V from the scorpion *Androctonus mauretanicus mauretanicus*. Toxicon **39**, 1579–1585

26 Bougis, P. E., Rochat, H. and Smith, L. A. (1989) Precursors of *Androctonus australis* scorpion neurotoxins. Structures of precursors, processing outcomes, and expression of a functional recombinant toxin II. J. Biol. Chem. **264**, 19259–19265

27 Ferrat, G., Bernard, C., Fremont, V., Mullmann, T. J., Giangiacomo, K. M. and Darbon, H. (2001) Structural basis for alpha-K toxin specificity for K^+ channels revealed through the solution 1H NMR structures of two noxiustoxin-iberiotoxin chimeras. Biochemistry **40**, 10998–10006

28 Pimenta, A. M. C., Stocklin, R., Favreau, P., Bougis, P. E. and Martin-Eauclaire, M. F. (2001) Moving pieces in a proteomic puzzle: mass fingerprinting of toxic fractions from the venom of *Tityus serrulatus* (Scorpiones, Buthidae). Rapid Commun. Mass Spectrum. **15**, 1562–1572

29 Cestele, S., Stankiewicz, M., Mansuelle, P., De Waard, M., Dargent, B., Gilles, N., Pelhate, M., Rochat, H., Martin-Eauclaire, M. F. and Gordon, D. (1999) Scorpion alpha-like toxins, toxic to both mammals and insects, differentially interact with receptor site 3 on voltage-activated sodium channels in mammals and insects. Eur. J. Neurosci. **11**, 975–985

30 Granier, C., Novotny, J., Fontecilla-Camps, J. C., Fourquet, P., el Ayeb, M. and Bahraoui, E. (1989) The antigenic structure of a scorpion toxin. Mol. Immunol. **26**, 503–513

31 Fontecilla-Camps, J. C., Habersetzer-Rochat, C. and Rochat, H. (1988) Orthorombic crystals and three-dimensional structure of the potent toxin II from the scorpion *Androctonus australis Hector*. Proc. Natl. Acad. Sci. U.S.A. **85**, 7443–7447

32 Pinheiro, C. B., Marangoni, S., Toyama, M. H. and Polikarpov, I. (2003) Structural analysis of *Tityus serrulatus* Ts1 neurotoxin at atomic resolution: insights into interactions with sodium channels. Acta Crystallogr. D Biol. Crystallogr. **59**, 405–415

33 Srairi-Abid, N., Mansuelle, P., Mejri, T., Karoui, H., Rochat, H., Sampieri, F. and El Ayeb, M. (2000) Purification, characterization and molecular modelling of two toxin-like proteins from the *Androctonus australis* Hector venom. Eur. J. Biochem. **267**, 5614–5620

34 Kharrat, R., Darbon, H., Rochat, H. and Granier, C. (1989) Structure/activity relationships of scorpion alpha-toxins. Multiple residues contribute to the interaction with receptors. Eur. J. Biochem. **181**, 381–390

35 Froy, O., Zilberberg, N., Gordon, D., Turkov, M., Gilles, N., Stankiewicz, M., Pelhate, M., Loret, E., Oren, D. A., Shaanan, B. and Gurevitz, M. (1999) The putative bioactive surface of insect-selective scorpion excitatory neurotoxins. J. Biol. Chem. **274**, 5769–5776

36 Bahraoui, E., El Ayeb, M., Van Rietschoten, J., Rochat, H. and Granier, C. (1986) Immunochemistry of scorpion alpha-toxins: study with synthetic peptides of the antigenicity of four regions of toxin II of *Androctonus australis Hector*. Mol. Immunol. **23**, 357–366

37 Devaux, C., Clot-Faybesse, O., Juin, M., Mabrouk, K., Sabatier, J. M. and Rochat, H. (1997) Monoclonal antibodies neutralizing the toxin II from *Androctonus australis* hector scorpion venom: usefulness of a synthetic, non-toxic analog. FEBS Lett. **412**, 456–460

38 Hamon, A., Gilles, N., Sautière, P., Martinage, A., Martinage, A., Kopeyan, C., Ulens, C., Tytgat, J., Lancelin, J.-M. and Gordon, D. (2002) Characterization of scorpion α-like toxin group using two new toxins from the scorpion *Leiurus quinquestriatus hebraeus*. Eur. J. Biochem. **269**, 3920–3933

39 Benzinger, G. R., Kyle, J. W., Blumenthal, K. M. and Hank, D. A. (1998) A specific interaction between the cardiac sodium channel and site-3 toxin Anthopleurin B. J. Biol. Chem. **273**, 80–84

Received 9 May 2003/1 August 2003; accepted 11 August 2003
Published as BJ Immediate Publication 11 August 2003, DOI 10.1042/BJ20030688

© 2003 Biochemical Society